Optimal sensor placement and motion coordination for target tracking

Sonia Martínez [a] Francesco Bullo [b]

[a] *Department of Mechanical and Aerospace Engineering, University of California, San Diego, CA, 92093-0411, USA*
Tel: (+1) 805 284-2564, Fax: (+1) 858 534-7078

[b] *Department of Mechanical and Environmental Engineering, University of California at Santa Barbara, Santa Barbara, CA, 93106-5070, USA*
Tel: (+1) 805 893-5169, Fax: (+1) 805 893-8651

Abstract

This work studies optimal sensor placement and motion coordination strategies for mobile sensor networks. For a target tracking application with range sensors, we investigate the determinant of the Fisher Information Matrix and compute it in the 2D and 3D cases, characterizing the global minima in the 2D case. We propose motion coordination algorithms that steer the mobile sensor network to an optimal deployment and that are amenable to a decentralized implementation. Finally, our numerical simulations illustrate how the proposed algorithms lead to improved performance of an extended Kalman filter in a target tracking scenario.

Key words: motion coordination, optimal sensor placement, Fisher Information Matrix, Kalman filtering.

1 Introduction

New advancements in the fields of microelectronics and miniaturization have generated a tremendous surge of activity in the development of sensor networks. The envisioned groups of agents are endowed with communication, sensing and computation capabilities, and promise great efficiency in the realization of multiple tasks such as environmental monitoring, exploratory missions and search and rescue operations. However, several fundamental problems need to be solved in order to make this technology possible. One main difficulty is the requirement for decentralized architectures where each agent takes autonomous decisions based on information shared with only a few local neighbors. Ongoing research work focuses on decentralized filters and data-fusing methods for estimation, and on the motion algorithms that guarantee the desired global behavior of the network. Ideally, both the motion control algorithms and estimation processes should be optimally integrated to make the most of the network performance.

Email addresses: soniamd@ucsd.edu (Sonia Martínez), bullo@engineering.ucsb.edu (Francesco Bullo).

In this paper we investigate the design of distributed motion coordination algorithms that increase the information gathered by a network in static and dynamic target-tracking scenarios. To do this, we define an aggregate cost function encoding a "sensitivity performance measure" and design our algorithms to maximize it. This idea has been widely used in papers on optimum experimental design for dynamical systems with applications to measurement problems. For example [8, 11] deal with problems on target tracking and parameter identification of distributed parameter systems. The motion control algorithms proposed in these papers either are computed via some off-line numerical method or are gradient algorithms. Often these algorithms are designed to maximize an appropriate scalar cost function and to choose the best sensor locations from a grid of finite candidates. Unfortunately, these schemes turn out to be not distributed since in order to define the control law for each agent, it is necessary to know all other agents' positions at each step. A second set of relevant references are those on distributed motion coordination. Our proposed control algorithms are in the same spirit of those of cyclic pursuit [6, 12], flocking [5], and coverage control [4].

The contributions of this paper are the following. Under the assumption of Gaussian noise measurements with

diagonal correlation, Section 2 presents closed-form expressions for the determinant of the Fisher Information Matrix for "range-measurement" models in non-random static scenarios, for 2 and 3 dimensional state spaces. This determinant plays the role of an objective function: we characterize its critical points in the 2D version and obtain sets of positions that globally maximize its value. If the sensors measure distances to the target, then an optimal configuration is one in which the sensors are uniformly placed in circular fashion around the target, confirming a natural intuition about the problem. Taking this optimal configuration as a starting point in Section 3, we then consider a target tracking scenario where the sensors move along the boundary of a convex set containing the target. We define discrete-time control laws that, relying only on local information, achieve the uniform configuration around the target (estimate) exponentially fast. In essence, our laws are very intuitive and simple-to-implement interaction behaviors between the sensors along the boundary. Finally, in Section 4, we numerically validate our coordination and optimal deployment laws in a particular dynamic target-tracking scenario. Although the network achieves global optimum configurations for a *nonrandom static* parameter estimation scenario, we simulate a *dynamic random* scenario. Our simulations illustrate the following reasonable conjecture: optimizing the sensitivity function for the static non-random case improves the performance of a filter (in our case an EKF) for the dynamic random scenario.

Finally, we point out that we assume that the process of estimation is performed by a central site or by a distributed process that we do not implement here. For works dealing with multisensor fusion possibly under communication constraints we refer to [9, 10] and references therein.

2 Optimal placement of sensors

Here we present the assumptions on our sensor network and target models in (1) (non-random) static estimation scenarios and (2) (random) dynamic parameter estimation scenarios. Other assumptions like those on the discrete motion of the sensors are given in Section 3. In this section, we obtain the corresponding Fisher Information Matrices (FIMs) for the estimation models and analyze the global minima of their determinant as a means to guarantee increased sensitivity with respect to the sensors' measurements. See [2] for a comprehensive treatment on estimation and tracking.

2.1 The static parameter estimation scenario

In what follows we consider ultrasound-based sensors, whose measurement model can be described as

$$z_i(q) = n_r h(\|p_i - q\|) + \eta_i + w_i\,,$$

where q is a point in the environment Q, n_r models the inverse sound-speed, η_i models the noise due to turbulence and w_i is a small white noise caused by the receiver at p_i. Here we assume that there is no noise due to turbulence and that $n_r = 1$ (this constant can be estimated by means of a filter). Finally, to include the feature that range measurements are usually trustworthy up to some limited range, we have affected $\|p_i - q\|$ by a function $h : [0, +\infty) = \mathbb{R}_+ \to \mathbb{R}$ (see Subsection 2.3). This model is inspired by those employed elsewhere in the literature, see for example [3, 13], and should be considered as a first, reasonable approximation of sensors providing time-of-flight measurements.

The localization of static targets can be solved as a non-random parameter estimation problem as follows. Let $p_j \in \mathbb{R}^d$, $j \in \{1, \ldots, n\}$, denote the position of n sensors moving in a convex region $Q \subseteq \mathbb{R}^d$ and let $q_0 \in Q$ be the unknown target position to be estimated by means of the measurement model:

$$z_j(q) = h(\|q - p_j\|) + w_j\,, \quad q \in Q\,, \tag{1}$$

for $j \in \{1, \ldots, n\}$. Here, w_j represents a zero mean white noise, $j \in \{1, \ldots, n\}$. The stacked vector of measurements at a given instant is a random vector normally distributed as

$$Z \triangleq \begin{bmatrix} z_1 \\ \vdots \\ z_n \end{bmatrix} \sim \mathcal{N}\left(\begin{bmatrix} h(\|q - p_1\|) \\ \vdots \\ h(\|q - p_n\|) \end{bmatrix}, R \right),$$

where $R = R^T > 0$ is the $n \times n$ covariance matrix. From now on, we use the shorthand notation $Z = (z_1, \ldots, z_n)^T$, and we let H denote the function $H(q, p_1, \ldots, p_n) = (h(\|q - p_1\|), \ldots, h(\|q - p_n\|))^T$.

The *Fisher Information Matrix* (FIM) for non-random parameters, denoted by J_{NR}, is defined as the expected value with respect to the probability distribution $p(Z|q)$:

$$J_{\text{NR}} \triangleq E\left[(\nabla_q \log \Lambda) \cdot (\nabla_q \log \Lambda)^T \right]_{q=q_0}\,,$$

where q_0 is the true value of the target location or an estimate of it, $\nabla_q = (\frac{\partial}{\partial q^1}, \ldots, \frac{\partial}{\partial q^d})^T$, and Λ is the *likelihood function*,

$$\Lambda(q, p_1, \ldots, p_n) = \frac{1}{\sqrt{2\pi \det R}} \exp\left(-\frac{1}{2}(Z - H)^T R^{-1} (Z - H) \right).$$

A few computations show $J_{\text{NR}} = (\nabla_q H)^T_{q_0} R^{-1} (\nabla_q H)_{q_0}$. Let $q = (q^1, \ldots, q^d)^T$, and define the shorthands

$$\partial_\ell h_j(q_0, p_1, \ldots, p_n) \triangleq \frac{\partial}{\partial q^\ell} h(\|q - p_j\|)\Big|_{q=q_0},$$

for $j \in \{1,\dots,n\}$ and $\ell \in \{1,\dots,d\}$. Then $(\nabla_q H)_{q_0} : \mathbb{R}^d \times (\mathbb{R}^n)^d \to \mathbb{R}^{n\times d}$ can be computed to be

$$((\nabla_q H)_{q_0})_{j\ell}(q_0, p_1, \dots, p_n) = \partial_\ell h_j(q_0, p_1, \dots, p_n)\,,$$

for $j \in \{1,\dots,n\}$ and $\ell \in \{1,\dots,d\}$. In the particular case that $R = \sigma^2 I_n$, the FIM $J_{\rm NR}$ can be expressed as:

$$\begin{aligned} J_{\rm NR}(q_0, p_1, \dots, p_n) &= \frac{1}{\sigma^2}(\nabla_q H)^T_{q_0}(\nabla_q H)_{q_0} \\ &= \frac{1}{\sigma^2}\sum_{j=1}^{n}\begin{bmatrix} (\partial_1 h_j)^2 & \dots & (\partial_1 h_j)(\partial_d h_j) \\ \vdots & \ddots & \vdots \\ (\partial_d h_j)(\partial_1 h_j) & \dots & (\partial_d h_j)^2 \end{bmatrix}. \end{aligned} \quad (2)$$

2.2 The dynamic parameter estimation scenario

Dynamic targets can be thought of as random parameters evolving under a stochastic difference equation. Here we assume that the target position $q(t)$ at time $t \in \mathbb{N}$ satisfies:

$$q(t) = F_t(q(t-1)) + v(t)\,, \quad q(0) \in Q\,,$$

for some functions $F_t : \mathbb{R}^d \to \mathbb{R}^d$ and $v(t)$ i.i.d as $v(t) \sim \mathcal{N}(0, N(t))$, where $N(t) = N(t)^T > 0$, for $t \geq 0$, and $E[v(i)v(j)^T] = \delta_{ij}N(i)$, for $i, j \in \mathbb{N}$. Similarly as before, we model our sensor network as

$$Z(t) = H_t(q(t), p_1(t), \dots, p_n(t)) + w(t), \quad t \geq 0,$$

with $H_t(q(t), p_1(t), \dots, p_n(t)) = (h_t(\|q(t) - p_1(t)\|), \dots, h_t(\|q(t) - p_n(t)\|))$, where $h_t : \mathbb{R}_+ \to \mathbb{R}$, and $Z(t) = (z_1(t), \dots, z_n(t))$, $t \geq 0$. We assume that $w(t) \sim \mathcal{N}(0, R(t))$, where $R(t) = R(t)^T > 0$, $t \geq 0$, and that $E[w(i)w(j)^T] = \delta_{ij}R(i)$, for $i, j \in \mathbb{N}$.

An estimation method that is widely employed for target tracking is that of the Extended Kalman Filter (EKF) [2]. The assumptions for the filter require $q(t)$ and $Z(t)$ to be jointly Gaussian distributed with covariance $P(t) = P(t)^T$, and $E[q(t)w(s)] = 0$, for $t, s \geq 0$. The EKF provides a state estimate $q_e(t)$ together with an estimate for the covariance of the error $P_e(t)$:

$$P_e(t) = P_p(t) - W(t)S(t)W(t)^T\,, \quad t \geq 1\,,$$

where $P_p(t)$ is the predicted covariance of the error and $W(t)$, $S(t)$ are some matrices appropriately defined [2]. Let $q_p(t)$ be the predicted value of $q(t)$. Some standard computations [2] allow us to say that

$$P_e^{-1}(t) = P_p^{-1}(t) + (\nabla_q H_{t|q_p(t)})^T R^{-1}(t)\nabla_q H_{t|q_p(t)}$$

or, denoting $(\nabla_q H_{t|q_p(t)})^T R^{-1}(t)\nabla_q H_{t|q_p(t)} = J_{\rm NR}(t)$,

$$P_e^{-1}(t) = P_p^{-1}(t) + J_{\rm NR}(t)\,, \quad t \geq 0\,. \quad (3)$$

Similarly, it can be seen that for linear measurement and linear target models, the FIM for dynamic (random) parameters, $J_{\rm DR}(t)$, and $J_{\rm NR}(t)$ satisfy

$$J_{\rm DR}(t) = J_{\rm NR}(t) + T(t)\,. \quad (4)$$

for some symmetric and positive definite matrix $T(t)$ such that $T(t)^{-1} = E[(q(t) - \bar{q}_t)(q(t) - \bar{q}_t)^T]$, with $\bar{q}_t = E[q(t)]$, $t \geq 1$.

2.3 Cost functions for optimal sensing

As is well known, the FIM encodes the "amount of information" that a set of measurements produces in estimating a set of parameters. Under the assumptions made in former sections, we have FIM = CRLB^{-1}; i.e., the FIM is the inverse of the Cramer Rao Lower Bound, which in turn lower bounds the covariance of the error

$$\text{FIM}^{-1} = \text{CRLB} \leq E[(\hat{q} - q_0)(\hat{q} - q_0)^T].$$

Because of this, one expects that "minimizing the CRLB" results in a decrease of uncertainty.

This line of reasoning has been a main theme in several papers dealing with *optimum experimental design* and *active sensing*, e.g., see [8, 11]. Starting from the FIM (resp. the CRLB) of the estimation approach, an *evaluation function* is defined (usually the determinant or the trace of the FIM/CRLB) whose maximization (resp. its minimization) is to be achieved. For example, the det FIM is the cost function in "D-optimum design" as discussed by [11].

As before, let $q_0 \in \mathbb{R}^d$ be the true value of the target location or an estimate of it. Under the assumptions of Subsection 2.1 and 2.2, we define our cost function $\mathcal{L}_{q_0} : (\mathbb{R}^d)^n \to \mathbb{R}_+$ by

$$\mathcal{L}_{q_0}(p_1, \dots, p_n) = \det J_{\rm NR}(q_0, p_1, \dots, p_n), \quad (5)$$

with $J_{\rm NR}$ given in (2). Because of (3) and (4), we are guaranteed that, if we optimize $\mathcal{L}_{q_0}$ with respect to the positions of the sensors, then we obtain increased performance in static estimation scenarios, and expect reasonably good performance in dynamic ones.

In what follows we derive the expression for the cost function $\mathcal{L}_{q_0}$ for $d = 2$ and $d = 3$ and analyze its critical points and global maxima. To do this, we shall assume that our measurement model is

$$h(r) = \begin{cases} (R_1 - c_1)^b + c_2, & r \geq R_1, \\ (r - c_1)^b + c_2, & R_0 < r < R_1, \\ (R_0 - c_1)^b + c_2, & r \leq R_0, \end{cases} \quad (6)$$

for $b \in \mathbb{Z}$, and constants $R_1 > R_0 > 0$, $c_2, c_1 \in \mathbb{R}_+$. Ultrasound sensors could be modeled in a first approximation by $b = 1$ and $c_1 = c_2 = 0$.

Proposition 2.1 *For $q_0 \in \mathbb{R}^d$, let $\mathcal{L}_{q_0} : (\mathbb{R}^d)^n \to \mathbb{R}_+$ be defined as in (5) and h be defined as in (6). Let $\mathcal{S}_{q_0}(p_1, \ldots, p_n)$ be the set of indices $i \in \{1, \ldots, n\}$ such that $R_0 < \|p_i - q_0\| < R_1$. The following statements hold true.*

(i) For $d = 2$,

$$\mathcal{L}_{q_0}(p_1, \ldots, p_n) = \frac{1}{2\sigma^2} \sum_{i,j \in \mathcal{S}_{q_0}} \|\mathbf{v}_i\|^2 \|\mathbf{v}_j\|^2 \sin^2 \alpha_{ij}$$

where $\alpha_{ij} \triangleq \measuredangle(\mathbf{v}_i, \mathbf{v}_j)$, $\mathbf{v}_i = (\partial_1 h_i, \partial_2 h_i, 0)$, and $\|\mathbf{v}_i\|^2 = b^2(\|p_i - q_0\| - c_1)^{2(b-1)}$, for $i, j \in \mathcal{S}_{q_0}(p_1, \ldots, p_n)$.

(ii) For $d = 3$,

$$\mathcal{L}_{q_0}(p_1, \ldots, p_n) = \frac{1}{6\sigma^2} \sum_{i,j,k \in \mathcal{S}_{q_0}} \|\mathbf{v}_i\|^2 \|\mathbf{v}_j\|^2 \|\mathbf{v}_k\|^2 \sin^2 \alpha_{ij} \cos^2 \beta_{ij,k}$$

where $\alpha_{ij} \triangleq \measuredangle(\mathbf{v}_i, \mathbf{v}_j)$, $\beta_{ij,k} \triangleq \measuredangle(\mathbf{v}_i \times \mathbf{v}_j, \mathbf{v}_k)$, and $\mathbf{v}_i = (\partial_1 h_i, \partial_2 h_i, \partial_3 h_i)$, with $\|\mathbf{v}_i\|^2 = b^2(\|p_i - q_0\| - c_1)^{2(b-1)}$, for $i, j, k \in \mathcal{S}_{q_0}(p_1, \ldots, p_n)$.

Here we understand that $\mathcal{L}_{q_0} = 0$ when $\mathcal{S}_{q_0} = \emptyset$.

The proof of this result is presented in the report [1].

Let us now introduce some useful notation. Let $\mathbb{T}$ be the circle in the plane and define $\mathcal{L}_{\mathbb{T}} : \mathbb{T}^n \to \mathbb{R}_+$ by

$$\mathcal{L}_{\mathbb{T}}(\delta_1, \ldots, \delta_n) = \frac{b^4 M^2}{2\sigma^2} \sum_{i,j=1}^{n} \sin^2(\delta_i - \delta_j),$$

where $M = \max_{r \in [R_0, R_1]} (r - c_1)^{2(b-1)} > 0$. Now, let $d = 2$ and assume $q_0 \neq p_i$, for $i \in \{1, \ldots, n\}$. Consider a polar change of coordinates centered at $q_0 \in \mathbb{R}^2$, and identify $p_i \in \mathbb{R}^2$ with (η_i, r_i) for some $\eta_i \in \mathbb{T}$ and $r_i \in \mathbb{R}_+$, $i \in \{1, \ldots, n\}$. Then, the following holds.

Lemma 2.2 *A necessary and sufficient condition for $(p_1, \ldots, p_n)$ to be a maximum of $\mathcal{L}_{q_0}$ is that:*

(a) $r_i \in \operatorname{argmax}_{r \in [R_0, R_1]} (r - c_1)^{2(b-1)}$, $\forall i \in \mathcal{S}_{q_0}$,
(b) $(\eta_1, \ldots, \eta_n) \in \operatorname{argmax} \mathcal{L}_{\mathbb{T}}$.

Proposition 2.3 *The following statements hold true.*

(i) The point $(\eta_1, \ldots, \eta_n) \in \mathbb{T}^n$ is a critical point for $\mathcal{L}_{\mathbb{T}}$ if either any two vectors in $\{(\cos 2\eta_i, \sin 2\eta_i)\}_{i=1}^n$ are aligned or

$$\sum_{i=1}^{n} \cos 2\eta_i = 0, \text{ and } \sum_{i=1}^{n} \sin 2\eta_i = 0,$$

(ii) The following three quantities are equal: $\frac{b^4 M^2}{4\sigma^2} n^2$, $\max\{\mathcal{L}_{q_0}(p_1, \ldots, p_n) \mid p_1, \ldots, p_n \in \mathbb{R}^d\}$, and $\max\{\mathcal{L}_{\mathbb{T}}(\delta_1, \ldots, \delta_n) \mid \delta_1, \ldots, \delta_n \in \mathbb{T}\}$.

(iii) If $\eta_i = (i-1)\pi/n$, $i \in \{1, \ldots, n\}$, then

$$\{(\eta_1 + k_1\pi, \ldots, \eta_n + k_n\pi) \mid k_1, \ldots, k_n \in \mathbb{Z}\}$$

are global maxima for $\mathcal{L}_{\mathbb{T}}$.

We refer to report [1] for a proof of these results.

Remark 2.4 *By (iii) there are global maxima with multiple sensors at the same position. This is related to our assumptions that the measurement noises w_j are uncorrelated. It is a conjecture that, if measurement noise is assumed to be positively correlated with nearby sensors locations, then maximum points have the feature that all sensors are at distinct locations.* •

We have compared the performance of static and optimally-placed sensors versus static and non-optimally placed sensors for estimating a static target in [1]. The simulations validate the results of this section. In Section 4 we compare the performance of moving versus static sensors, which is the case of interest for us.

3 Motion coordination algorithms for sensor reconfiguration about static targets

This section presents a family of decentralized control laws that steers the sensors to a set of points of maximum for a particular class of costs functions previously defined. Specifically, we focus here on functions corresponding to measurement models with $h(r) = r$. Our analysis is related to the approaches in [4, 5, 6, 12]. We make the following assumptions on the defining elements of our problem:

(i) a static target q_0 takes values in the interior of a compact convex set Q with static boundary ∂Q known by each sensor;
(ii) each of the sensors $\{p_1, \ldots, p_n\}$ moves in discrete time along ∂Q;
(iii) each of the sensors $\{p_1, \ldots, p_n\}$ detects its immediate clockwise and counterclockwise neighbors in ∂Q and acquires the corresponding distances.

For this static scenario with limited information, the motion coordination objective is to steer $\{p_1, \ldots, p_n\}$ to the equally-spaced angular positions around the target q_0 exponentially fast. There is no estimation process here;

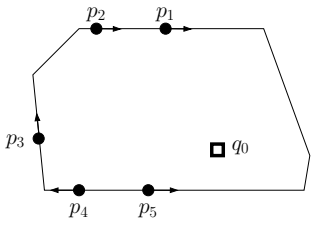

Fig. 1. Assumptions (i) and (iii): the sensors move along the boundary of a fixed Q and the target moves inside Q.

the algorithm will be incorporated later as part of the estimation filter and coordination algorithm in Section 4.

Remark 3.1 *Assumption (iii) means that an implementable control law for an agent can only depend on the agent's position relative to its neighbors (in the natural ring topology along ∂Q). We call such a control law* spatially distributed along ∂Q. •

3.1 From the boundary of Q to a circle and back

Because we take $h(r) = r$, an optimal configuration $(p_1, \ldots, p_n)$ satisfies condition (a) of Lemma 2.2. In other words, in order to find an optimal configurations of the sensors, we only need to adjust their polar coordinates about the target q_0. Since the region Q is a convex set, we can just focus on these polar coordinates and define the motion control strategies on a circle.

Let ∂Q be implicitly defined by the continuous equation $x \in \partial Q$ if and only if $g(x) = 0$. Given a point q in the interior of a compact convex set Q, define the map $\varphi_q : \partial Q \to \mathbb{T}$ by

$$\varphi_q(p) = \frac{p - q}{\|p - q\|}.$$

One can show that φ_q is continuous with continuous inverse $\varphi_q^{-1} : \mathbb{T} \to \partial Q$ given by $\varphi_q^{-1}(v) = q + \lambda v$ where $\lambda \in \mathbb{R}_+$ the unique solution to $g(q + \lambda p) = 0$. We illustrate the map φ_q in the following figure.

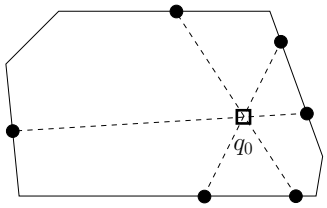

Fig. 2. Six sensors with angular configuration equally spaced about the point q_0.

In what follows, we let q_0 denote the current estimate of the target location, we let $\varphi_{q_0}(p)$ be the angular component of the polar coordinates of p centered at q_0, and we identify $p_i \in \partial Q \subset \mathbb{R}^2$ with $\eta_i = \varphi_{q_0}(p_i) \in \mathbb{T}$, for all i.

3.2 Basic behaviors for uniform coverage of the circle

As discussed, the location of the sensors is described by the vector $(\eta_1, \ldots, \eta_n)$ of elements of $\mathbb{T}$. We assume that angles are measured counterclockwise and that the sensors are placed in counterclockwise order (we adopt the convention that $\eta_{n+1} = \eta_1$ and that $\eta_0 = \eta_n$).

As described in Assumption (iii), the sensors motion is described by a discrete-time control system:

$$\eta_i(t+1) = \eta_i(t) + u_i, \quad i \in \{1, \ldots, n\}.$$

Here u_i is the scalar control magnitude of the ith sensor. In a way consistent with Assumption (iv), we assume that u_i is a function only of the relative angular distances in the counterclockwise direction $d_{\text{counterclock},i} = \eta_{i+1} - \eta_i > 0$ and clockwise direction $d_{\text{clock},i} = \eta_i - \eta_{i-1} > 0$. We also assume that each sensor obeys the same motion control law $u : [0, 2\pi] \times [0, 2\pi] \to \mathbb{R}$, so that the closed-loop system becomes:

$$\begin{aligned} \eta_i(t+1) &= \eta_i(t) + u(d_{\text{counterclock},i}(t), d_{\text{clock},i}(t)), \\ d_{\text{counterclock},i}(t) &= \eta_{i+1}(t) - \eta_i(t), \\ d_{\text{clock},i}(t) &= \eta_i(t) - \eta_{i-1}(t). \end{aligned}$$

In order to achieve uniform distribution of the sensors on the circle, two simple behaviors arise fairly naturally, see Figure 3. First, we consider the Go towards the midpoint behavior with $u_{\text{midpoint}} : [0, 2\pi] \times [0, 2\pi] \to \mathbb{R}$

$$u_{\text{midpoint}}(d_{\text{counterclock}}, d_{\text{clock}}) = \frac{1}{2}\big(d_{\text{counterclock}} - d_{\text{clock}}\big).$$

The interpretation is clear: each sensor moves towards the midpoint of the angular segment between the preceding and following sensor. In the original coordinate system, each sensor moves along ∂Q towards the bisector of the triangle with vertex q_0 and vertices given by the preceding and following sensor. A second intuitive rule

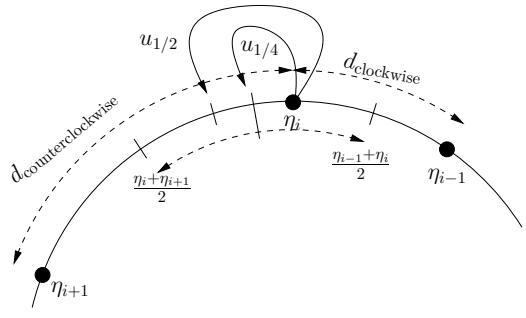

Fig. 3. The Go towards the midpoint $u_{1/2}$ and Go towards the midpoint of Voronoi segment $u_{1/4}$ behaviors.

is the Go towards the midpoint of Voronoi seg-

MENT behavior $u_{\text{midpoint Voronoi}} : [0, 2\pi] \times [0, 2\pi] \to \mathbb{R}$

$$u_{\text{midpoint Voronoi}}(d_{\text{counterclock}}, d_{\text{clock}}) = \frac{1}{4}(d_{\text{counterclock}} - d_{\text{clock}}).$$

The interpretation is the following: the Voronoi segment of the ith sensor at position η_i is the angular segment from $(\eta_{i-1} + \eta_i)/2$ to $(\eta_i + \eta_{i+1})/2$, and the control law GO TOWARDS THE MIDPOINT OF VORONOI SEGMENT steers η_i towards the midpoint of this segment.

These two rules are particular instances of the following family of linear algorithms parametrized by $\kappa \in \mathbb{R}$:

$$u_\kappa(d_{\text{counterclock}}, d_{\text{clock}}) = \kappa(d_{\text{counterclock}} - d_{\text{clock}}).$$

Clearly, u_{midpoint} and $u_{\text{midpoint Voronoi}}$ are equal to u_κ for $\kappa = 1/2$ and $\kappa = 1/4$, respectively. Because $u_\kappa(d, d) = 0$ for all $d \in \mathbb{R}_+$, the equally-spaced angle position (where the sensors are uniformly distributed around the target) is an equilibrium point [1] for the u_κ-closed-loop system.

3.3 Convergence analysis

To perform a convergence analysis, it is convenient to define the relative angular distances $d_i = \eta_{i+1} - \eta_i$, for $i \in \{1, \dots, n\}$ (and adopt the usual convention that $d_{n+1} = d_1$ and that $d_0 = d_n$). So long as the counterclockwise order of the sensors is not violated, we have $(d_1, \dots, d_n) \in S_{2\pi} = \{x \in \mathbb{R}_n \mid x_i \geq 0, \sum_{i=1}^n x_i = 2\pi\}$. The change of coordinates from $(\eta_1, \dots, \eta_n)$ to $(d_1, \dots, d_n)$ and the control law u_κ jointly lead to the closed-loop system

$$d_i(t+1) = \kappa d_{i+1}(t) + (1 - 2\kappa)d_i(t) + \kappa d_{i-1}(t).$$

This is a linear time-invariant dynamical system with state $d = (d_1, \dots, d_n)$, transition matrix A_κ given by

$$\begin{bmatrix} 1-2\kappa & \kappa & 0 & \cdots & 0 & \kappa \\ \kappa & 1-2\kappa & \kappa & \ddots & \ddots & 0 \\ 0 & \kappa & 1-2\kappa & \ddots & \ddots & \vdots \\ \vdots & \ddots & \ddots & \ddots & \ddots & 0 \\ 0 & \ddots & \ddots & \kappa & 1-2\kappa & \kappa \\ \kappa & 0 & \cdots & 0 & \kappa & 1-2\kappa \end{bmatrix},$$

and governing equation

$$d(t+1) = A_\kappa d(t), \quad \text{for } t \in \mathbb{N} \cup \{0\}. \tag{7}$$

[1] The more general linear feedback $u(d_{\text{counterclock}}, d_{\text{clock}}) = ad_{\text{counterclock}} + bd_{\text{clock}}$ does not have the desired equilibrium set unless $a + b = 0$. The case of $a + b \neq 0$ is studied in the context of cyclic pursuit, see [6] and references therein.

Theorem 3.2 *The control law u_κ is spatially distributed along ∂Q, and, for $\kappa \in]0, 1/2[$, the solutions to the corresponding closed-loop system (7) preserve the counterclockwise order of the sensors and converge exponentially fast to $(2\pi/n, \dots, 2\pi/n)$.*

Proof. Recall the notion and properties of circulant matrices from [7]. Since A_κ is circulant with representer $p_{A_\kappa}(s) = (1 - 2\kappa) + \kappa s + \kappa s^{n-1}$, its eigenvalues are

$$\lambda_\ell = p_{A_\kappa}\Big(\exp\big(\frac{2\pi\ell\sqrt{-1}}{n}\big)\Big) = 1 - 2\kappa + 2\kappa\cos\big(\frac{2\pi\ell}{n}\big),$$

for $\ell \in \{1, \dots, n\}$. Observe that $\lambda_n = 1$ with eigenvector $\mathbf{1}^T = (1, \dots, 1)$. If $\kappa > 0$ and $\ell \in \{1, \dots, n-1\}$, then

$$-1 \leq \cos\big(\frac{2\pi\ell}{n}\big) < 1 \quad \Longrightarrow \quad 1 - 4\kappa \leq \lambda_\ell < 1.$$

Therefore, if $\kappa \in]0, 1/2[$, then $\lambda_1, \dots, \lambda_{n-1}$ belong to the interval $]-1, 1[$. Additionally, if $\kappa \in]0, 1/2[$, then A_κ is a doubly-stochastic matrix, which implies that $S_{2\pi}$ is invariant for A_κ.

Let $\{\mathbf{e}_1, \cdots, \mathbf{e}_{n-1}, \mathbf{1}\}$ be a basis of orthogonal eigenvectors for A_κ corresponding to $\{\lambda_1, \dots, \lambda_n\}$, respectively. Any initial condition $d(0)$ can be written as

$$d(0) = \sum_{\ell=1}^{n-1} \rho_\ell \mathbf{e}_\ell + \rho_n \mathbf{1}\,.$$

Since $\sum_{i=1}^n d_i(0) = 2\pi$, then $\rho_n = \frac{2\pi}{n}$. Therefore

$$d(t) = A_\kappa d(t-1) = \sum_{\ell=1}^{n-1} \lambda_\ell^t \rho_\ell\, \mathbf{e}_\ell + \frac{2\pi}{n}\mathbf{1}\,.$$

If $\kappa \in]0, 1/2[$, then each $|\lambda_\ell| < 1$, for $\ell \in \{1, \dots, n-1\}$ and, therefore, each trajectory $t \mapsto d(t)$ converges to $\frac{2\pi}{n}\mathbf{1}$, the equal-angle configuration, exponentially fast.

Remark 3.3 *(i) The properties of u_κ in Theorem 3.2 are independent of the number n of sensors.*

(ii) If $\kappa < 0$ or $\kappa > 1/2$, then there exist initial conditions from which the counterclockwise order of the sensors is not preserved in the closed loop.

(iii) Consider the $\kappa = 1/2$ case, corresponding to the GO TOWARDS THE MIDPOINT *behavior. Although* GO TOWARDS THE MIDPOINT *is a very natural algorithm to consider, it does* not *ensure convergence to the desired configuration whenever n is even. In fact, if $n = 2L$ with $L \in \mathbb{Z}$, then $\mathbf{1}$ and $\mathbf{e}_L^T = (-1, 1, -1, \dots, -1, 1)$ are eigenvectors with eigenvalues 1 and -1 respectively. Given $\{\mathbf{e}_1 \dots, \mathbf{e}_{n-1}, \mathbf{1}\}$ an orthogonal basis of eigenvectors for $A_{1/2}$ and $d(0) = \sum_{i=1}^{n-1} \rho_i \mathbf{e}_i + \rho_n \mathbf{1}$, one can show that, starting*

from arbitrary initial conditions, the system exponentially converges to a steady oscillation between $\mathbf{u}_1 = \rho_n \mathbf{1} + \rho_L \mathbf{e}_L$ *and* $\mathbf{u}_2 = \rho_n \mathbf{1} - \rho_L \mathbf{e}_L$. •

4 Target tracking simulations with Kalman filtering and motion coordination algorithms

Here we combine the developments of the former sections and we define the Active Target Tracking algorithm for collective improved sensing performance. We numerically simulate the algorithm to validate our approach. It is assumed that the estimation step is carried out after a round of communication has taken place to propagate all the measurements taken among the agents.The algorithm is summarized in the following table.

Name: ACTIVE TARGET TRACKING ALGORITHM

Goal: Decentralized motion coordination of sensors and joint localization of target

Data: (i) Constant $\kappa \in]0, 1/2[$.
(ii) Equation for the boundary of the containment region, $g(q) = 0$.
(iii) Guess for target position $\hat{q}_0(0)$.

At time t, local agent $i \in \{1, \ldots, n\}$ performs:

1: Receive estimate $\hat{q}_0(t)$ from fusion center.
2: Detect counterclockwise and clockwise neighbors along ∂Q, compute angular distances in polar coordinates about $\hat{q}_0(t)$.
3: Compute control u_κ, next desired position $\eta_i(t+1) \in \mathbb{T}$, and corresponding point $p_i(t+1) \in \partial Q$.
4: Move to new position $p_i(t+1)$ along ∂Q.
5: Take new measurement of target $z_i(t+1)$, and send it to fusion center, that updates target estimate according to EKF.

In what follows we present our numerical results. We compare the estimation errors of the trajectory of a dynamic target; we assume that measurements are taken from a set of four stationary or four moving sensors. For the purpose of the simulation, Q is a disk centered at the origin with radius $1.5m$, and the target trajectory is the eight-shaped curve:

$$\begin{bmatrix} q_0^1(t) \\ q_0^2(t) \end{bmatrix} = \begin{bmatrix} \sin(\omega t) \\ \sin(\omega t)\cos(\omega t) \end{bmatrix}, \qquad t \geq 0\,.$$

Here (q_0^1, q_0^2) are measured in meters and $\omega = .1$ Hz.

In the following two figures, the plots compare the evolution of the absolute error trajectories along time, $E(t) = \|q_0(t) - \hat{q}_0(t)\|$ for stationary sensors (dashed red line) and moving sensors (solid blue line), for $t \geq 0$. The first set of simulations, see Figure 4, illustrates the results obtained for four sensors initially positioned at 2.1818, 2.4500, 3.7160, and 4.5167 radians. As can be seen, the moving sensors perform better on average as the variance increases. In the second set of simulations, see

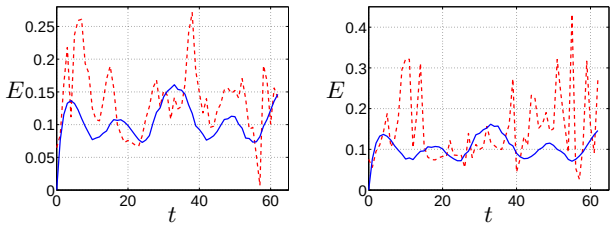

Fig. 4. Evolution of absolute error trajectories with variances of measured noise 5×10^{-3} (left) and 5×10^{-2} (right).

Figure 5, we take as the sensors initial position the optimal position to estimate $\mathbf{0}$. That is, 0, $\pi/2$, π and $3\pi/2$, are the initial positions for both stationary and moving sensors. Although the set of moving sensors performs

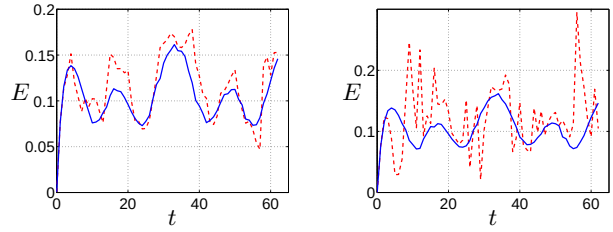

Fig. 5. Evolution of absolute error trajectories with variances of measured noise 5×10^{-2} (left) and 10^{-1} (right).

better, the differences between the estimates of the stationary and moving sensors are comparable for measurement variances of order 10^{-3}, 10^{-2} (the absolute error trajectories overlap). When the measurement noise is in the order of 10^{-1}, there is a clear difference in performance. Qualitatively, Figure 6 shows how the trajectory estimated by the moving sensors (green solid line) behaves as compared with the trajectory estimated by the stationary sensors (black dashed line). The actual target trajectory is so close to the green solid estimated trajectory that we do not plot it. In all the simulations, the variance of the process noise is of the order of 10^{-5}; for larger values of the process noise the performance of moving versus stationary sensors is comparable.

5 Conclusions and future work

We have presented novel decentralized control laws for the optimal positioning of sensor networks that track a target. It would be of clear interest to modify our model by including upper bounds on the motion and detection range of the sensors. Broader future research lines include (1) the consideration of heterogeneous collections

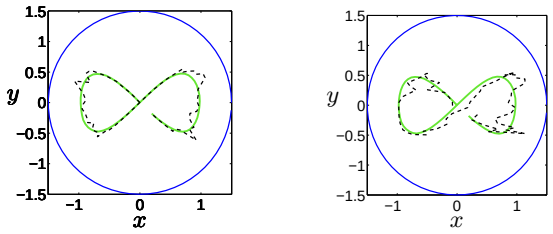

Fig. 6. Qualitative evolution of the estimated trajectories by moving and stationary sensors. Initial positions are $(0, \pi/2, \pi, 3\pi/2)$ (left) and $(2.1818, 2.4500, 3.7160, 4.5167)$ (right) and variances are in both cases 5×10^{-2}.

of sensors, (2) the dynamic assignment of sensors to different targets and (3) investigation of decentralized estimation and fusion schemes.

Acknowledgements

This material is based upon work supported in part by ONR YIP Award N00014-03-1-0512 and NSF SENSORS Award IIS-0330008. Sonia Martínez's work was partially supported by a Fulbright Postdoctoral Fellowship from the Spanish Ministry of Education and Culture.

References

[1] S. Aranda, S. Martínez, and F. Bullo. On optimal sensor placement and motion coordination for target tracking. Technical Report CCEC-04-1013, CCDC. University of California at Santa Barbara, 2004.

[2] Y. Bar-Shalom, X. R. Li, and T. Kirubarajan. *Estimation with Applications to Tracking and Navigation*. John Wiley & Sons, New York, NY, 2001. ISBN 047141655X.

[3] G. Benet, F. Blanes, J. E. Simó, and P. Pérez. Using infrared sensors for distance measurement in mobile robots. *Robotics and Autonomous Systems*, 40(4):255–266, 2002.

[4] J. Cortés, S. Martínez, T. Karatas, and F. Bullo. Coverage control for mobile sensing networks. *IEEE Transactions on Robotics and Automation*, 20(2):243–255, 2004.

[5] A. Jadbabaie, J. Lin, and A. S. Morse. Coordination of groups of mobile autonomous agents using nearest neighbor rules. *IEEE Transactions on Automatic Control*, 48(6):988–1001, 2003.

[6] J. A. Marshall, M. E. Broucke, and B. A. Francis. Formations of vehicles in cyclic pursuit. *IEEE Transactions on Automatic Control*, 49(11):1963– 1974, 2004.

[7] C. D. Meyer. *Matrix Analysis and Applied Linear Algebra*. SIAM, Philadelphia, PA, 2001. ISBN 0898714540.

[8] B. Porat and A. Nehorai. Localizing vapor-emitting sources by moving sensors. *IEEE Transactions on Signal Processing*, 44(4):1018–1021, 1996.

[9] B. S. Y. Rao, H. F. Durrant-Whyte, and J. S. Sheen. A fully decentralized multi-sensor system for tracking and surveillance. *International Journal of Robotics Research*, 12(1):20–44, 1993.

[10] B. Sinopoli, L. Schenato, M. Franceschetti, K. Poolla, M. I. Jordan, and S. S. Sastry. Kalman filtering with intermittent observations. *IEEE Transactions on Automatic Control*, 49(9):1453–63, 2004.

[11] D. Uciński. *Optimal Measurement Methods for Distributed Parameter System Identification*. CRC Press, Boca Raton, FL, 2004. ISBN 0849323134.

[12] I. Wagner and A. M. Bruckstein. Row straightening by local interactions. *Circuits, Systems and Signal Processing*, 16(3):287–305, 1997.

[13] H. W. Wehn and P. R. Belanger. Ultrasound-based robot position estimation. *IEEE Transactions on Robotics and Automation*, 13(5):682–692, 1997.